Micron 174 (2023) 103533

Contents lists available at ScienceDirect

Micron

journal homepage: www.elsevier.com/locate/micron

Durability assessment of hydrogel mountings for contrast-enhanced micro-CT

Torben Hildebrand [a,*], Jan Novak [a,c], Liebert Parreiras Nogueira [b], Aldo Roberto Boccaccini [c], Håvard Jostein Haugen [a]

[a] Department of Biomaterials, Institute of Clinical Dentistry, Faculty of Dentistry, University of Oslo, Oslo 0317, Norway
[b] Oral Research Laboratory, Institute of Clinical Dentistry, Faculty of Dentistry, University of Oslo, Oslo 0317, Norway
[c] Department of Materials Science and Engineering, Friedrich-Alexander-Universität, 91054 Erlangen, Germany

ARTICLE INFO

Keywords:
Contrast enhancement
Drosophila melanogaster
Iodine
Phosphotungstic acid
Poloxamer 407
Agarose

ABSTRACT

Micro-computed tomography (micro-CT) provides valuable data for studying soft tissue, though it is often affected by sample movement during scans and low contrast in X-ray absorption. This can result in lower image quality and geometric inaccuracies, collectively known as 'artefacts'. To mitigate these issues, samples can be embedded in hydrogels and enriched with heavy metals for contrast enhancement. However, the long-term durability of these enhancements remains largely unexplored. In this study, we examine the effects of two contrast enhancement agents – iodine and phosphotungstic acid (PTA) – and two hydrogels – agarose and Poloxamer 407 – over a 14-day period. We used *Drosophila melanogaster* as a test model for our investigation. Our findings reveal that PTA and agarose are highly durable, while iodine and poloxamer hydrogel exhibits higher leakage rates. These observations lay the foundation for estimating contrast stabilities in contrast-enhanced micro-CT with hydrogel embedding and serve to inform future research in this field.

1. Introduction

For micro-CT image acquisition, samples must be mounted between the X-ray source and detector. The sample is rotated during scanning to generate 2D-projections for the 3D-reconstruction. Small movements of the samples during the image acquisition can lead to blurring as well as small movements or shifts in the image (du Plessis et al., 2017) and, therefore result in compromised image quality. Geometrical inaccuracies can be caused by not adequately secured sample loading (du Plessis et al., 2017) but also due to shrinkage, especially during long scans (du Plessis et al., 2017; Sasov et al., 2008). Soft tissues in high-resolution imaging are prone to such instabilities and threaten image quality by being complicated to mount and having a high potential for shrinkage. Small samples are commonly mounted in supportive embedding systems such as hydrogels (Hong et al., 2020; Kavkova et al., 2021; Liao et al., 2023; Senter-Zapata et al., 2016; Vymazalova et al., 2017), paraffin wax, or resins (Sengle et al., 2013; Senter-Zapata et al., 2016) to assure physical stability. However, embedding in the latter systems can affect the feasibility of further analysis of the samples. Still, it can also lead to sample shrinkage and structural distortion due to dehydration associated with the embedding protocol, such as wax embedding (Senter-Zapata et al., 2016).

Hydrogel embedding allows scanning in an aqueous environment, preventing sample shrinkage. This can improve the image resolution despite the slightly increased X-ray attenuation of the hydrogel (Hong et al., 2020). In particular, agarose of concentrations up to 2 % is a widely used hydrogel (Hong et al., 2020; Kavkova et al., 2021; Liao et al., 2023; Senter-Zapata et al., 2016; Vymazalova et al., 2017). Using agarose, the hydrogel is liquefied by heating above 60 °C, which may affect the sample to embed. Compared to agarose, Poloxamer 407 hydrogels show an inverse thermo-response, meaning, specifically in this case, that the reversible gelation is initiated by increasing the temperature. Depending on the polymer concentration, the gel is formed at room temperature (Gioffredi et al., 2016). Using thermo-sensitive hydrogels such as from Poloxamer 407 reduces the embedding temperatures significantly without adding other substances to ensure

Abbreviations: Br, brain; CE, contrast enhancement; CR, contrast ratio; CT, computed tomography; DLM, dorso-longitudinal muscles; GV, Grey value; I_2E, iodine in ethanol; PTA, phosphotungstic acid; RCR, relative contrast ratio; VNC, ventral nerve cord.

* Corresponding author.
E-mail address: torbehil@odont.uio.no (T. Hildebrand).

https://doi.org/10.1016/j.micron.2023.103533
Received 25 July 2023; Received in revised form 17 August 2023; Accepted 28 August 2023
Available online 29 August 2023

mounting stability during the scan.

Besides physical stability during scanning, soft tissues show a low inherent contrast in X-ray absorption micro-CT due to the low X-ray attenuation, making the method unusable for accessing structural information of non-mineralised tissue (de et al., 2015; Heimel et al., 2019). Various contrast enhancement protocols have been developed to address the challenge of the low contrast of soft tissue. These protocols utilise different chemical agents containing heavy metal elements capable of binding to the tissue of interest. Iodine-based solutions or phosphotungstic acid hydrate formulas are widely utilised for contrast-enhanced micro-CT and were first described by Metscher (Metscher, 2009a, 2009b). However, the effect of time after embedding in combination with the use of contrast enhancement agents is crucial to be investigated. Concerning high-resolution scans and the associated scan duration or preparation in advance for use in another facility, a scan or series of scans cannot be executed in a timely, affecting the image quality or contrast of the structure to be analysed. Here, we used male *Drosophila melanogaster* as a test model for assessing contrast stability for contrast-enhanced micro-CT using iodine- and PTA-based agents in agarose and Poloxamer 407 hydrogel mounting over 14 days. *Drosophila melanogaster* is a widely studied model organism that finds applications in diverse disciplines, including human brain disease research (Jeibmann and Paulus, 2009) and increasingly in cancer research (Mirzoyan et al., 2019). Recently, micro-CT imaging has emerged as a valuable tool for anatomical and developmental characterization of *Drosophila*, as demonstrated by Schoberg et al. (Schoborg et al., 2019). Staining procedures have been individually optimized (Schoborg et al., 2019; Smith et al., 2016; Sombke et al., 2015) with a shared goal of enhancing contrast, whereby the durability of the contrast enhancement was not considered.

The aim of the study is to elaborate on differences in the durability of contrast in contrast-enhanced micro-CT depending on a) the used staining agent and its solvent and b) the embedding hydrogel. Based on the results, our objective is to identify the optimal combination of staining agent and hydrogel for future experiments of a similar nature while also establishing a foundation for evaluating the durability of other combinations.

2. Materials and methods

2.1. Sample preparation

Male *Drosophila melanogaster* (n = 8) were carefully fixed using 70 % ethanol (VWR International SAS, Rosny-sous-Bois, France). The samples were then divided into two groups for further treatment. Half of the samples were gradually adapted to distilled water in 10 % increments, with each step lasting 30 min. Meanwhile, the other half was separated into two additional groups: one remained in 70 % ethanol, while the other was gradually adapted to 100 % ethanol in 10 % steps, each step lasting 30 min.

The samples immersed in water were subjected to two different staining procedures: either immersed in 1 % (w/v) PTA (Phosphotungstic acid, Sigma-Aldrich, St. Louis, MO, USA) solution in water (PTA-H_2O) for a duration of 5 days or treated with a 1.5 % (w/v) Lugol's solution (iodine (Sigma-Aldrich, St. Louis, MO, USA) and potassium iodide (Sigma-Aldrich, St. Louis, MO; USA) in a ratio of 1:2) for a period of 3 days. The samples preserved in 70 % ethanol were immersed in a 1 % PTA solution in 70 % ethanol (PTA-E) for 5 days, while the samples adapted to 100 % ethanol were treated with a 1 % iodine solution in 100 % ethanol for 3 days, also further abbreviated as I_2E.

The abdomens of the samples treated with PTA were gently punctured beforehand using a microneedle. This puncturing allowed for faster penetration of the staining agent into the samples.

2.2. Micro-computed tomography (Micro-CT)

The treated samples underwent rinsing using either 70 % or 100 % ethanol for ethanol-based contrast enhancement, while water was used for water-based contrast-enhanced samples. Subsequently, the specimens were embedded in 1 % (w/v) low-melt agarose (Bio-Rad Laboratories, Hercules, CA, USA) or 25 % (w/v) Poloxamer 407 with a molecular weight of 12.6 kDa (Pluronic F-127, Sigma-Aldrich, St. Louis, MO, USA) in deionized water. The embedding process involved direct placement of the treated samples within a sealed 200-µL pipette tip (Mettler-Toledo Rainin, Oakland, CA, USA) for CT-mounting. The head of the *Drosophila melanogaster* pointed towards the sealed opening of the pipette tip.

All the prepared specimens were scanned using a micro-CT system (SkyScan 1172, Bruker micro-CT, Kontich, Belgium) at 55 kV, 160 µA, and an exposure time of 700 ms over a 360° rotation with a rotation step of 0.37°. These settings resulted in a final voxel size of 2.15 µm. Scans for each sample were performed directly after embedding and after 1, 2, 3, 4, 7 and 14 days. The scanning process for each sample lasted approximately 40 min.

After the scanning, micro-CT projections were reconstructed using the system-provided software NRecon (version 1.7.4.6), which included ring artefact correction 6 and beam hardening correction of 50 %. The resulting reconstructions were then visualised and analysed using the software Dragonfly (Object Research Systems (ORS), Montréal, Canada, version 2022.1).

3. Theory/calculation

3.1. Contrast ratio

Three tissues of the fruit fly were segmented from the obtained data sets of each scan: brain (Br), dorso-longitudinal muscles (DLM), and the ventral nerve cord (VNC), as illustrated in Fig. 1. Additionally, two spheres with a diameter of 250 µm were segmented containing the embedding hydrogel. One has been selected in front and one in the back of the fruit fly.

Grey values of the mentioned tissues (GV_S) and of the surrounding embedding system (GV_B) were quantified by averaging from the segmented volumes. The contrast ratio (CR) from the scan directly after embedding was calculated by the given formula (Swart et al., 2016) (Eq. 1):

$$CR = (\overline{GV_S} - \overline{GV_B}\ )/\overline{GV_B} \quad (1)$$

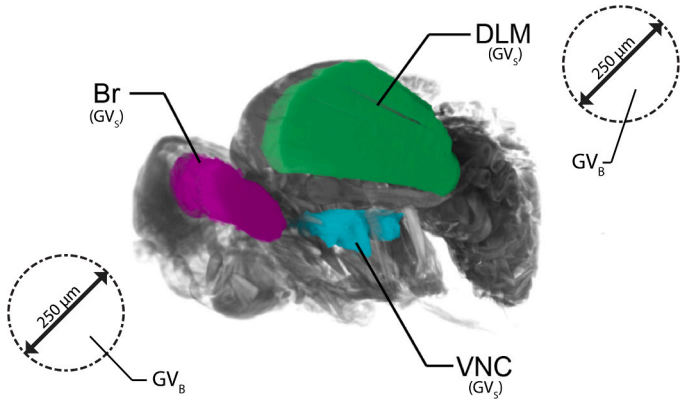

Fig. 1. Schematic illustration of the three segmented tissues of *Drosophila melanogaster* : Br (purple), DLM (green) and VNC (cyan) and the two spherical segmentations representing the embedding hydrogel.

3.2. Relative contrast ratio over time

The relative contrast ratio was calculated after 1, 2, 3, 4, 7, and 14 days with the corresponding scan by formula (Eq. 2):

$$RCR_d = 1 - ((\overline{GV_{d0}} - \overline{GV_d})/\overline{GV_{d0}}) \quad (2)$$

Where RCR_d represents the relative contrast ratio observed after d days, $\overline{GV_{d0}}$ denotes the mean grey value of the considered structures on day 0, and $\overline{GV_d}$ signifies the mean grey value of the same tissues after d days have passed.

4. Results

The grey values of the embedding systems, namely $GV_{B,1\%Agarose}$ and $GV_{B,25\%Pluronic}$ remained consistent across all scans and were quantified as 29.28 ± 0.28 and 28.95 ± 0.44, respectively. No significant differences can be found between these values. Measurable trends over time and differences in sampling in front and the back of the sample could not be observed.

4.1. Contrast ratio

The contrast ratios for each combination of contrast enhancement agent and embedding hydrogel were calculated using formula (1) and are presented in Table 1 for iodine-based contrast agents and Table 2 for PTA-based contrast agents. Notably, the PTA-based contrast enhancement consistently demonstrated higher contrast ratios than the iodine-based one. Within the iodine-based contrast enhancements, Lugol's iodine exhibited higher contrast ratios in both embedding hydrogels when compared to ethanol-based iodine.

The analysis of contrast ratios within the PTA-based contrast enhancement did not indicate major differences among the four tested systems.

4.2. Relative contrast ratio over time

Relative contrast for days 1–4, days 7 and 14 shown in Fig. 2 were calculated according to formula (2). Fig. 2 shows each combination of contrast enhancement agent and embedding hydrogel. Iodine-based contrast enhancement in agarose- and poloxamer embedding indicated higher losses in relative contrast than PTA-based preparations. Agarose embedding and ethanol-based contrast solutions showed lower contrast losses than poloxamer embedding and water-based contrast solutions. Especially measurements on day 1 showed already this tendency. Whereas I_2E contrast enhancement in agarose embedding showed no remarkable decrease in contrast, Lugol's iodine with poloxamer embedding dropped by about 16.2 % in relative contrast. From day 2 to day 14 all combinations showed a steady decrease in contrast, whereby the slope of the decrease with poloxamer embeddings was greater. After a span of 14 days, a consistent trend became more pronounced: the combination of ethanol-based staining and agarose embedding exhibited the smallest decrease in relative contrast, with a decline of 22 %. Following closely was the combination of Lugol's iodine staining and agarose embedding, which showed the second-lowest decline at 38 %. Ethanol-based staining paired with poloxamer embedding resulted in a relative contrast drop of 48 %, while the highest decrease of 63 % was observed with Lugol's iodine staining combined with poloxamer embedding.

Table 1
Mean of contrast ratios (CR) and standard deviations (SD) from examined tissues for iodine-based contrast-enhanced measurements.

	I_2E: Agarose	I_2E: Poloxamer	Lugol's iodine: Agarose	Lugol's iodine: Poloxamer
CR	1.37	0.98	1.89	1.83
SD	0.16	0.14	0.24	0.18

Table 2
Mean of contrast ratios (CR) and standard deviations (SD) from examined tissues for PTA-based contrast-enhanced measurements.

	PTA-E: Agarose	PTA-E: Poloxamer	PTA-H_2O: Agarose	PTA-H_2O: Poloxamer
CR	3.13	2.73	3.27	3.41
SD	0.51	0.34	0.37	0.20

The utilisation of PTA in water for contrast enhancement, in combination with agarose embedding, exhibited a more substantial decrease in contrast over time compared to the other combinations. However, the reduction of relative contrast after 14 days is only 17 %.

Fig. 3 illustrates representative cross-sections of *Drosophila melanogaster* at days 0 and 14 after contrast enhancement in their embedding hydrogel. All representative cross-sections for iodine-based contrast enhancement (Appendix 1) and PTA-based contrast enhancement (Appendix 2), including the intervening time points, are available in the supplements. Qualitatively, the contrasts of iodine-based contrast enhancement after 14 days decreased much stronger than PTA-based contrast enhancement. In particular, embedding in 25 % poloxamer showed low contrasts after 14 days. Additionally, when poloxamer embedding was combined with PTA-based contrast enhancement, a notable decrease in the homogeneity of the contrast enhancement, indicated by lamps of higher attenuation, was observed. In comparison, such uniformity could not be found in agarose embeddings.

5. Discussion

Contrast-enhanced micro-CT techniques often utilize hydrogel embedding, especially agarose, to minimize the risk of sample displacement, which may affect image quality. Despite its benefits, the durability of contrast enhancement within hydrogel embedding still needs to be explored, an issue that becomes critical when scans cannot be conducted immediately post-sample preparation.

Our study used *Drosophila melanogaster* as a test model to examine the influence of two contrast enhancement agents – iodine and phosphotungstic acid – used in water and ethanol and two embedding materials – agarose and Poloxamer 407. This comprehensive approach resulted in four key findings: (1) The water content primarily influences the hydrogels' attenuation. (2) Iodine-based contrast decreases faster than phosphotungstic acid-based contrast. (3) There is a significant decrease in relative contrasts with poloxamer embedding compared to agarose embedding. (4) Iodine-based contrast enhancements show lower durability when water is used as the solvent.

Initially, in all of the eight examined systems of contrast agent and hydrogel, the contrast of the brain (Br), dorso-longitudinal muscles (DLM), and the ventral nerve cord (VNC) of the *Drosophila melanogaster* was sufficient for segmentation. The embedding hydrogel type does not significantly influence the contrast between the organ and background.

PTA-based contrast enhancement provides more remarkable contrasts than iodine-based ones, which was also reported in a similar study (Swart et al., 2016). This is explained by the higher atomic number of tungsten ($Z(I) = 53$; $Z(W) = 74$) which leads to higher contrast enhancement, as demonstrated by Pauwels et al. in a comparison of 28 different contrast agents (Pauwels et al., 2013). However, the affinity and amount of bound contrast agent to the tissue must also be addressed as possible factors. Lugol's iodine provided a greater contrast than I_2E among iodine-based contrast enhancement, although the used concentration of iodine was lower than in I_2E. Therefore, it is assumed that water and/or the potassium iodide facilitate the iodine accumulation within the sample tissue. PTA-based contrast enhancement did not reveal any significant differences due to the presence of either water or ethanol.

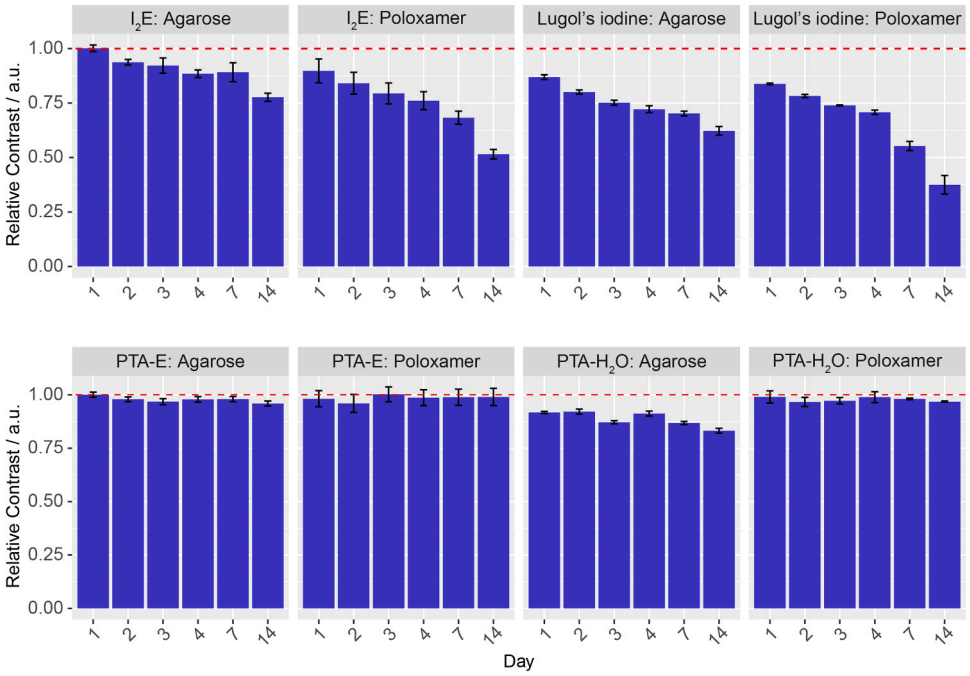

Fig. 2. Relative contrast ratio over 14 days for both iodine-based (top row) and PTA-based (bottom row) contrast enhancement methods. The contrast ratios were measured for both agarose and poloxamer embedding techniques. The values correspond to the individual grey values of day 0, which were set to 1.00 for each respective combination (dashed line).

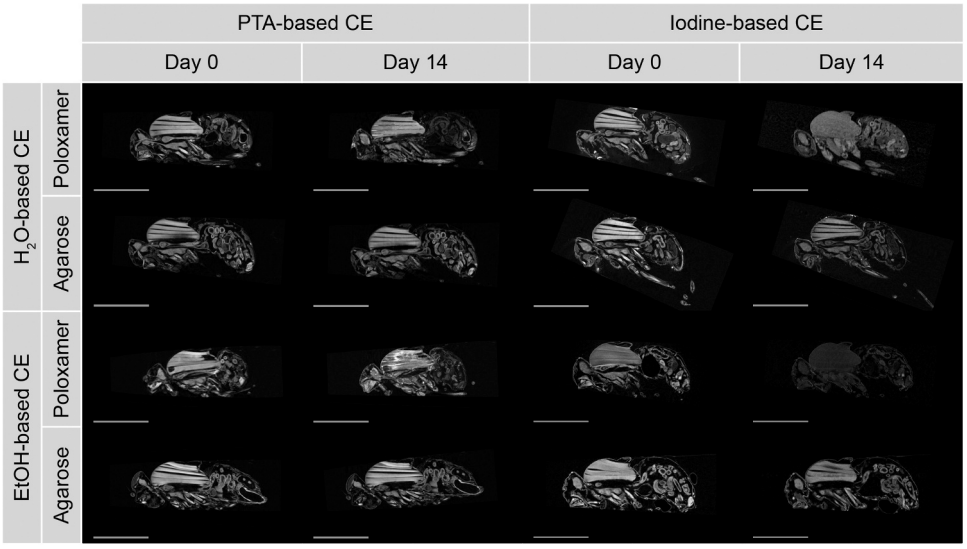

Fig. 3. Representative cross-sectional images of PTA- and iodine-based contrast enhancement (CE) in agarose and poloxamer embedding at days 0 and 14. Scale bar: 1 mm.

Iodine-based contrast enhancement exhibited a higher decrease in relative contrast and, thusly stronger leakage than PTA-based contrast enhancement. Iodine, more precisely I_2 and I_3^- (the latter is present in Lugol's iodine), are smaller molecules than PTA with smaller hydrodynamic radiuses and hence higher mobility and diffusibility (Schoborg et al., 2019). They penetrate samples quicker but also diffuse out of the sample within shorter periods. The lower loss of relative contrast of PTA-based contrast enhancement is likewise explainable by the larger molecule size of PTA molecules. Furthermore, differences in the binding affinity and its mechanisms could contribute to the observed variation in durability on contrast enhancement, demanding consideration as potential contributing factors. It is assumed that the preparation method plays an additional role. PTA-contrast enhanced samples were punctured to ensure infiltration since PTA cannot penetrate the cuticle of *Drosophila melanogaster* (Schoborg et al., 2019). Consequently, there is only one opening for PTA molecules to diffuse out of the sample, reducing the leakage.

The influence of poloxamer on leakage behaviour is particularly noticeable among iodine-based contrast enhancements. Poloxamer 407 as embedding hydrogel seems to increase the leakage rate of iodine out of the tissue compared to agarose. The used poloxamer hydrogel appears to attract the iodine's contrast medium stronger than agarose. This could be due to the high concentration of poloxamer (25 % (w/v)) compared to a low agarose concentration (1 % (w/v)). A higher diffusion gradient of water/ethanol is the consequence, leading to increased leakage of the also included contrast agent. However, for more stable contrast

enhancements or samples that do not require contrast enhancement, poloxamer hydrogels continue to be an excellent choice for micro-CT embedding due to their numerous advantageous properties including good processability.

Besides the embedding hydrogel, water as a solvent for contrast enhancement exhibited higher leakage rates than ethanol. This is demonstrated within iodine-treated samples to a higher extent than with PTA contrast enhancement. The enhanced solubility of iodine in water in the presence of potassium iodide (Varlamova et al., 2009) from the contrast solution can explain the increased absorption in the embedding hydrogel. Preparation with iodine in ethanol for contrast enhancement did not insert potassium iodide into the embedding system. Hence, the slight solubility of iodine hindered the leakage from the sample into the hydrogel.

The study's objective was to evaluate contrast-enhanced micro-CT's durability when using hydrogel mountings. The methodology involved examining eight different systems, including four staining protocols and two hydrogels. However, it is important to note that this selection does not encompass all possible embedding hydrogels or staining agents, limiting the generalizability of the findings. The time period of 14 days showed a major change in contrast for iodine-based contrast enhancements. Change in contrast for PTA-treated samples is indicated to be lower. However, qualitatively cross-sections demonstrated an increasingly affected homogeneity of contrast enhancement using PTA in combination with poloxamer as embedding hydrogel. Nevertheless, other combinations might not show a measurable impact on the sampling rate used here.

The broad design of the tests introduces the possibility of systematic errors, as the number of samples analysed may not fully account for all potential influences. Here, it is worth mentioning that the protocols involving PTA required the puncturing of the abdomen, which may introduce additional considerations or limitations of the used test model in combination with PTA.

Furthermore, it should be acknowledged that the test model used in this study represents a simplified model, and its applicability to other sample types may be limited or require further investigation.

6. Conclusions

In the realm of contrast-enhanced micro-CT imaging, our study sought to investigate the durability of contrast enhancement agents, specifically iodine and Phosphotungstic acid (PTA), and the efficacy of two hydrogels, agarose and Poloxamer 407, as mounting methods. This research was conducted using a *Drosophila melanogaster* test model.

We found that PTA demonstrate d superior durability as a contrast enhancement agent when compared to iodine. This was observed regardless of the hydrogel used, poloxamer or agarose. Iodine-based contrast enhancement experienced leakage after just one day, with Lugol's iodine causing a decrease in contrast exceeding 12 %.

Among the hydrogels, agarose displayed higher durability than poloxamer. Our results also indicate that combining ethanol as the solvent for contrast enhancement with agarose as the embedding system resulted in optimal durability, particularly when PTA was employed as the contrast agent. This combination enabled structural analysis for over a week. On the other hand, samples stained in PTA with water as a solvent and embedded in Poloxamer 407, retained acceptable quality for several days.

These findings underscore the necessity of carefully selecting appropriate contrast agents and embedding systems to ensure reliable and long-lasting contrast-enhanced micro-CT imaging. Our study contributes valuable information to this field, particularly in the context of preparing samples using hydrogel mountings. This method offers several advantages despite its potential to compromise image quality.

Declaration of Competing Interest

The authors declare that they have no known competing financial interests or personal relationships that could have appeared to influence the work reported in this paper.

Data availability

Data will be made available on request.

Appendix A. Supporting information

Supplementary data associated with this article can be found in the online version at doi:10.1016/j.micron.2023.103533.

References

de, S. e S.J.M., Zanette, I., Noel, P.B., Cardoso, M.B., Kimm, M.A., Pfeiffer, F., 2015. Three-dimensional non-destructive soft-tissue visualization with X-ray staining micro-tomography. Sci. Rep. 5, 14088. https://doi.org/10.1038/srep14088.

du Plessis, A., Broeckhoven, C., Guelpa, A., le Roux, S.G., 2017. Laboratory x-ray micro-computed tomography: a user guideline for biological samples. Gigascience 6 (6), 1–11. https://doi.org/10.1093/gigascience/gix027.

Gioffredi, E., Boffito, M., Calzone, S., Giannitelli, S.M., Rainer, A., Trombetta, M., Mozetic, P., Chiono, V., 2016. Pluronic F127 hydrogel characterization and biofabrication in cellularized constructs for tissue engineering applications. Procedia CIRP 49, 125–132. https://doi.org/10.1016/j.procir.2015.11.001.

Heimel, P., Swiadek, N.V., Slezak, P., Kerbl, M., Schneider, C., Nurnberger, S., Redl, H., Teuschl, A.H., Hercher, D., 2019. Iodine-enhanced Micro-CT imaging of soft tissue on the example of peripheral nerve regeneration. Contrast Media Mol. Imaging 2019, 7483745. https://doi.org/10.1155/2019/7483745.

Hong, S.H., Herman, A.M., Stephenson, J.M., Wu, T., Bahadur, A.N., Burns, A.R., Marrelli, S.P., Wythe, J.D., 2020. Development of barium-based low viscosity contrast agents for micro CT vascular casting: application to 3D visualization of the adult mouse cerebrovasculature. J. Neurosci. Res. 98 (2), 312–324. https://doi.org/10.1002/jnr.24539.

Jeibmann, A., Paulus, W., 2009. Drosophila melanogaster as a model organism of brain diseases. Int. J. Mol. Sci. 10 (2), 407–440. https://doi.org/10.3390/ijms10020407.

Kavkova, M., Zikmund, T., Kala, A., Salplachta, J., Proskauer Pena, S.L., Kaiser, J., Jezek, K., 2021. Contrast enhanced X-ray computed tomography imaging of amyloid plaques in Alzheimer disease rat model on lab based micro CT system. Sci. Rep. 11 (1), 5999 https://doi.org/10.1038/s41598-021-84579-x.

Liao, W.N., You, M.S., Ulhaq, Z.S., Li, J.P., Jiang, Y.J., Chen, J.K., Tse, W.K.F., 2023. Micro-CT analysis reveals the changes in bone mineral density in zebrafish craniofacial skeleton with age. J. Anat. 242 (3), 544–551. https://doi.org/10.1111/joa.13780.

A Metscher, B.D., 2009a. MicroCT for developmental biology: a versatile tool for high-contrast 3D imaging at histological resolutions. Dev. Dyn.: Off. Publ. Am. Assoc. Anat. 238 (3), 632–640.

Metscher, B.D., 2009b. MicroCT for comparative morphology: simple staining methods allow high-contrast 3D imaging of diverse non-mineralized animal tissues. BMC Physiol. 9, 11. https://doi.org/10.1186/1472-6793-9-11.

Mirzoyan, Z., Sollazzo, M., Allocca, M., Valenza, A.M., Grifoni, D., Bellosta, P., 2019. Drosophila melanogaster: a model organism to study cancer. Front. Genet. 10, 51 https://doi.org/10.3389/fgene.2019.00051.

Pauwels, E., Van Loo, D., Cornillie, P., Brabant, L., Van Hoorebeke, L., 2013. An exploratory study of contrast agents for soft tissue visualization by means of high resolution X-ray computed tomography imaging. J. Microsc. 250 (1), 21–31. https://doi.org/10.1111/jmi.12013.

Sasov, A., Liu, X., Salmon, P., 2008. Compensation of mechanical inaccuracies in micro-CT and nano-CT, Vol. 7078. SPIE. https://doi.org/10.1117/12.793212.

Schoborg, T.A., Smith, S.L., Smith, L.N., Morris, H.D., Rusan, N.M., 2019. Micro-computed tomography as a platform for exploring Drosophila development. Development 146 (23). https://doi.org/10.1242/dev.176685.

Sengle, G., Tufa, S.F., Sakai, L.Y., Zulliger, M.A., Keene, D.R., 2013. A correlative method for imaging identical regions of samples by micro-CT, light microscopy, and electron microscopy: imaging adipose tissue in a model system. J. Histochem Cytochem 61 (4), 263–271. https://doi.org/10.1369/0022155412473757.

Senter-Zapata, M., Patel, K., Bautista, P.A., Griffin, M., Michaelson, J., Yagi, Y., 2016. The role of micro-CT in 3D histology imaging. Pathobiology 83 (2–3), 140–147. https://doi.org/10.1159/000442387.

Smith, D.B., Bernhardt, G., Raine, N.E., Abel, R.L., Sykes, D., Ahmed, F., Pedroso, I., Gill, R.J., 2016. Exploring miniature insect brains using micro-CT scanning techniques. Sci. Rep. 6, 21768 https://doi.org/10.1038/srep21768.

Sombke, A., Lipke, E., Michalik, P., Uhl, G., Harzsch, S., 2015. Potential and limitations of X-Ray micro-computed tomography in arthropod neuroanatomy: a methodological and comparative survey. J. Comp. Neurol. 523 (8), 1281–1295. https://doi.org/10.1002/cne.23741.

Swart, P., Wicklein, M., Sykes, D., Ahmed, F., Krapp, H.G., 2016. A quantitative comparison of micro-CT preparations in Dipteran flies. Sci. Rep. 6, 39380 https://doi.org/10.1038/srep39380.

Varlamova, T.M., Rubtsova, E.M., Mushtakova, S.P., 2009. Solubility diagrams of the potassium iodide-water-ethanol and iodine-water-ethanol ternary systems. Russ. J. Phys. Chem. A 83 (11), 1896–1899. https://doi.org/10.1134/s0036024409110156.

Vymazalova, K., Vargova, L., Zikmund, T., Kaiser, J., 2017. The possibilities of studying human embryos and foetuses using micro-CT: a technical note. Anat. Sci. Int. 92 (2), 299–303. https://doi.org/10.1007/s12565-016-0377-3.